CONCENTRATION POLARIZATION IN AN ULTRAFILTERING CAPILLARY

WILLIAM M. DEEN, CHANNING R. ROBERTSON, *and* BARRY M. BRENNER

From the Kidney Research Laboratory, Veterans Administration Hospital, San Francisco, California 94121, the Department of Chemical Engineering, Stanford University, Stanford, California 94305, and the Department of Medicine, University of California, San Francisco, California 94143

ABSTRACT Concentration polarization, the accumulation of retained solute next to an ultrafiltering membrane, elevates osmotic pressure above that which would exist in the absence of polarization. For ultrafiltration in a cylindrical tube, use of the radially averaged solute concentration results in an underestimate of osmotic pressure, yielding an effective hydraulic permeability (k) less than the actual membrane hydraulic permeability (k_m). The extent to which k and k_m might differ in an ultrafiltering capillary has been examined theoretically by solution of the momentum and species transport equations for idealized capillaries with and without erythrocytes. For diameters, flow velocities, protein concentrations and diffusivities, and ultrafiltration pressures representative of the rat glomerular capillary network, results indicate that the effects of polarization are substantial without erythrocytes ($k/k_m = 0.7$) and persist, but to a lesser extent, with erythrocytes ($k/k_m = 0.9$), the reduction in polarization in the latter case being due to enhanced plasma mixing. In accord with recent experimental findings in rats, k is found to be relatively insensitive to changes in glomerular plasma flow rate.

INTRODUCTION

Ultrafiltration and reverse osmosis both involve the use of an applied pressure to cause solvent flow through a semipermeable membrane in a direction opposite to normal osmotic flow. Whether the solutes retained by the membrane are macromolecules (e.g., proteins) as in ultrafiltration, or smaller solutes (e.g., NaCl) as in reverse osmosis, the rate of fluid exchange is governed by the transmembrane hydraulic and osmotic pressure differences:

$$V_w = k_m(\Delta P - \Delta\pi). \quad (1)$$

In Eq. 1, which holds for an ideal semipermeable membrane, V_w is the transmembrane fluid flux, k_m is the membrane hydraulic permeability, and ΔP and $\Delta\pi$ are the transmembrane hydraulic and osmotic pressure differences, respectively. In capil-

laries, where ultrafiltration is also governed by Eq. 1, $\Delta\pi$ is the colloid osmotic pressure of the plasma proteins.

A problem commonly encountered in the operation of commercial ultrafiltration and reverse osmosis systems is the accumulation of retained solutes next to the semipermeable membrane. This phenomenon, known as "concentration polarization," results from solute being transported to the membrane by bulk motion of the fluid. The solute concentration at the membrane increases until, in the steady state, the rate of solute diffusion away from the membrane equals the rate of convective transport toward it. Concentration polarization may reduce the efficiency of the separation process by (*a*) lowering the solvent flux due to increased osmotic pressure (which depends on the solute concentration only at the membrane), (*b*) increasing solute concentration in the filtrate (if solute rejection by the membrane is incomplete), or both. It is of interest, because of the demonstrated importance of concentration polarization in nonbiological ultrafiltration and reverse osmosis systems, to determine whether this phenomenon plays a significant part in governing transcapillary fluid exchange rates.

Concentration polarization in the microcirculation is most likely to be encountered where ultrafiltration rates are highest, as in the renal glomerular capillaries (1). Recent experimental advances have allowed glomerular ultrafiltration to be characterized in single mammalian nephrons by measurement of hydraulic and colloid osmotic pressures, and flow rates in a variety of physiological and pathophysiological states (2–8). A one-dimensional model of glomerular ultrafiltration (9), in which protein concentration is a function only of axial distance along an idealized capillary, has been employed in the interpretation of these experimental results (3–8). Since, as was pointed out in a recent review (1), this model does not allow for radial concentration gradients within a capillary, its use to compute glomerular hydraulic permeability from experimental data in the rat (5, 8) gives an "effective" value which reflects not only the resistance offered by the glomerular capillary wall but also the mass transfer resistance due to polarization. Hence, the effective hydraulic permeability (k) should be less than the true membrane permeability (k_m), the difference between k and k_m depending on the amount of polarization actually present.

In certain ultrafiltration systems the retained macromolecules may be concentrated sufficiently to exceed the solubility limit and thereby form a gel structure on the membrane surface, creating in effect an additional membrane barrier (10). This may be a serious problem because, ultimately, a point may be reached where further increases in applied pressure do not increase the solvent flux, but only add proportionately to the gel thickness or density (10). It is apparent from the measured values of ΔP in glomerular capillaries (2–8) that intracapillary protein concentration cannot exceed approximately 10 g/100 ml (compared with the systemic value of 6 g/100 ml) without cessation of ultrafiltration. Since the solubility limit

for serum albumin has been measured to be 58.5 g/100 ml (11), gel formation is unlikely to be a factor in glomerular ultrafiltration. Nevertheless, the ratio k/k_m may be substantially less than unity. Estimation of the probable value of k/k_m in a glomerular capillary requires that an analysis be made of the convection and diffusion of protein within such a capillary.

Kozinski and Lightfoot (11, 12) have studied concentration polarization in protein ultrafiltration with a view toward prediction of the onset of gel formation, and in an effort to develop mass transfer correlations for the design of ultrafiltration systems. Their analyses, however, employ boundary layer approximations not applicable to the low Reynolds number flow in a capillary. The numerous analyses of polarization in reverse osmosis systems, reviewed recently by Gill et al. (13), do not take into account a number of features peculiar to protein ultrafiltration, including the highly nonlinear dependence of osmotic pressure on protein concentration.[1] An additional unique feature of protein ultrafiltration in capillaries is the two-phase nature of capillary blood flow (plasma and erythrocytes). Thus, while polarization has been examined extensively, the available analyses are not readily applicable to the present problem of estimating k/k_m in a capillary.

Two idealized, steady flow models of capillary ultrafiltration will be utilized in this study to examine the possible effects of concentration polarization. In the first of these, the "bolus" model, segments of plasma are assumed to be trapped between successive erythrocytes, which are modeled as discs of the same diameter as the capillary. This idealization, first suggested by Prothero and Burton (14), has been used several times as a model of blood flow in narrow capillaries (15–18). Of importance, transcapillary fluid exchange was assumed to be zero (15–18). The second case to be considered, the "tube" model, neglects the presence of red blood cells and therefore, by comparison with the bolus model, allows estimation of the degree to which plasma motion induced by red cells might influence the amount of polarization. The results indicate that the modest extent of polarization predicted for glomerular capillaries is sufficient to yield k/k_m values appreciably less than one under some circumstances, but that this effect is minimized by the presence of erythrocytes.

LIST OF SYMBOLS

a_1, a_2 Empirical constants in Eq. 9, mm Hg/(g/100 ml) and mm Hg/(g/100 ml)^2, respectively.

A_1, A_2 Dimensionless osmotic pressure coefficients, $a_1C_0/\Delta P$ and $a_2C_0^2/\Delta P$, respectively.

b_1, b_2 Dimensionless parameters, $\Delta P/a_1C_0$ and a_2C_0/a_1, respectively.

β Dimensionless erythrocyte spacing in bolus model.

c Dimensionless protein concentration, C/C_0.

[1] Kozinski and Lightfoot (11, 12) considered, in addition to a nonlinear osmotic pressure, variations in viscosity and diffusivity with protein concentration. These properties will be considered constant in the present study, because of the limited range of protein concentrations encountered in capillaries.

C Protein concentration, g/100 ml.
D Protein diffusivity, cm²/s.
E^2 $\left(\frac{\partial^2}{\partial r^2} - \frac{1}{r}\frac{\partial}{\partial r} + \frac{\partial^2}{\partial z^2}\right)$ operator.
k Effective hydraulic permeability, cm/(s·mm Hg).
k_m Membrane hydraulic permeability, cm/(s·mm Hg).
L Length of idealized capillary, cm.
μ Fluid viscosity, g/(cm·s).
ΔP Transmembrane hydraulic pressure difference, mm Hg.
Pe Péclet number, U_0R/D.
Pe_w Wall Péclet number, $V_{w_0}R/D$.
$\Delta\pi$ Transmembrane colloid osmotic pressure difference, mm Hg.
ϕ Defined by Eq. 27.
ψ Stream function, defined by Eq. 11.
r Dimensionless radial distance ($0 \leq r \leq 1$).
R Radius of idealized capillary, cm.
ρ Density of plasma, g/cm³.
Re Reynolds number, $\rho U_0R/\mu$.
t Dimensionless time (characteristic time = R/U_0).
θ Extent of concentration polarization, Eq. 28.
u Dimensionless axial velocity, U/U_0.
U Axial velocity, cm/s.
v Dimensionless radial velocity, V/U_0.
V Radial velocity, cm/s.
x Dimensionless axial distance from tube inlet ($0 \leq x \leq L/R$).
z Dimensionless axial coordinate in plasma segment between erythrocytes ($0 \leq z \leq \beta$).

Superscripts

— Mean value.
⌢ Transformed variable.

Subscripts

0 Initial or initial mean value.
w Value at capillary wall, $r = 1$.

MODEL DEVELOPMENT

Bolus Flow

When the diameter of a capillary is smaller than that of a red cell, plasma is essentially trapped between successive red cells. The bolus flow model idealizes this situation by treating the red cells as solid plugs around which there is negligible plasma leakage. The geometry corresponding to the bolus model is shown in Fig. 1, in which two red cells in a cylindrical capillary are separated by a plasma space of dimensionless length β, which has been normalized by R, the capillary radius. In a coordinate system in which red cell 1 is considered to be stationary, the capillary wall is in motion with dimensionless velocity u_w, normalized with respect to the initial wall velocity, U_0. The radial (r) and axial (z) coordinates originate on the tube centerline at red cell 1, as shown. The unique feature of the present problem is that as

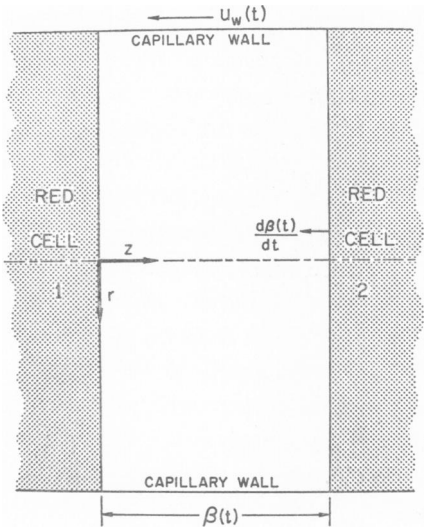

FIGURE 1

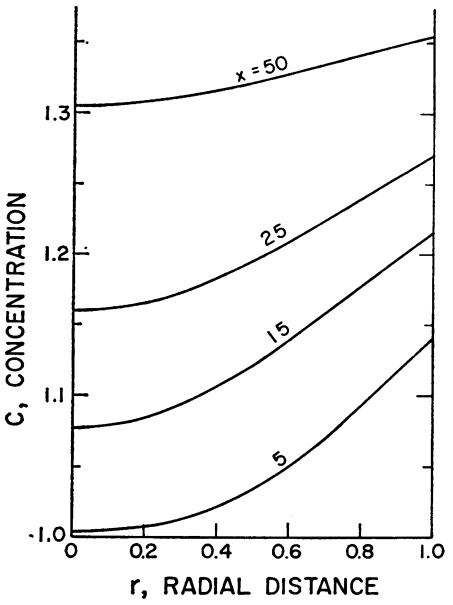

FIGURE 2

FIGURE 1 Coordinate system for bolus flow model.
FIGURE 2 Radial concentration profile as a function of axial distance (x) for tube flow model (Pe = 50, Pe_w = 0.301, b_1 = 3.58, b_2 = 1.08).

fluid is lost from the plasma space by ultrafiltration, the red cells decelerate and approach one another (that is, u_w and β decrease). Thus, red cell 2 moves with velocity $d\beta/dt$ with respect to red cell 1. In this reference frame the dimensionless time coordinate (t), normalized with R/U_0, is related to the "macroscopic" distance (x) the cells move along the capillary:

$$x = \int_0^t u_w \, dt', \tag{2}$$

where the distance x is measured from the beginning of the permeable capillary. The quantities β, $d\beta/dt$, and u_w are in general all functions of t.

In this analysis of concentration polarization, it is necessary to solve three interrelated sets of equations: (a) those expressing conservation of protein at a point (species transport), (b) those dealing with the fluid motion (momentum transport), and (c) the overall balance (macroscopic) equations for fluid volume, protein, and erythrocytes.

The species transport equation for a system without chemical reaction, in dimensionless form, is (19):

$$Pe\left[\frac{\partial c}{\partial t} + u\frac{\partial c}{\partial z} + v\frac{\partial c}{\partial r}\right] = \frac{\partial^2 c}{\partial r^2} + \frac{1}{r}\frac{\partial c}{\partial r} + \frac{\partial^2 c}{\partial z^2}, \tag{3}$$

where c is the protein concentration (normalized by C_0, the systemic protein concentration), u is the axial (z) and v the radial (r) component of velocity, Pe is the Péclet number (U_0R/D), and D is the protein diffusivity. Note that the time-dependent and convective transport terms are on the left side of Eq. 3, while the diffusive terms appear on the right. Since the dimensionless variables have been defined so that their magnitudes are presumed to be of ordre unity (abbreviated 0[1]), and since Pe multiplies the convective terms, the value of Pe is a measure of the relative importance of convective and diffusive transport of protein. For the protein concentrations of interest, the diffusivity of serum albumin (at 37°C) can be estimated from the data of Keller et al. (20) to be some 7×10^{-7} cm²/s. Assuming D, the effective diffusivity for the mixture of albumin and globulins in plasma, to be similar to this value, and estimating U_0 and R to be approximately 10^{-1} cm/s and 4×10^{-4} cm, respectively, Pe is approximately 50 for protein in a capillary. It may be expected, therefore, that the fluid motion will have an appreciable effect on the distribution of protein within the plasma.

The initial and boundary conditions corresponding to Eq. 3 for the bolus problem shown in Fig. 1 are:

$$c = 1 \text{ at } t = 0, \tag{4}$$

$$\partial c/\partial z = 0 \text{ at } z = 0, \beta(t), \tag{5}$$

$$\partial c/\partial r = 0 \text{ at } r = 0, \tag{6}$$

$$\partial c/\partial r = Pe\, v_w c \text{ at } r = 1. \tag{7}$$

Eq. 4 expresses the assumption of uniform concentration at the instant ultrafiltration begins, while Eqs. 5–7 specify no net flux of protein across any of the boundaries. The radial velocity at the permeable wall, v_w, is given by a dimensionless form of Eq. 1:

$$v_w = \frac{Pe_w}{Pe}\left(\frac{b_1 - c - b_2 c^2}{b_1 - 1 - b_2}\right), \tag{8}$$

where $Pe_w = V_{w_0}R/D$, $V_{w_0} = k_m(\Delta P - a_1C_0 - a_2C_0^2)$ (the dimensional ultrafiltration flux at $t = 0$), $b_1 = \Delta P/a_1C_0$, and $b_2 = a_2C_0/a_1$. The constants a_1 and a_2 arise from an empirical equation giving $\Delta\pi$ in terms of C_w (dimensional):

$$\Delta\pi = a_1C_w + a_2C_w^2. \tag{9}$$

For C_w between 4 and 10 g/100 ml, $a_1 = 1.629$ mm Hg/(g/100 ml) and $a_2 = 0.2935$ mm Hg/(g/100 ml)² (9, 21). Eq. 7, written in terms of the dimensionless parameters Pe_w, b_1, and b_2, becomes:

$$\frac{\partial c}{\partial r} = Pe_w \left(\frac{b_1 - c - b_2 c^2}{b_1 - 1 - b_2} \right) c \quad \text{at} \quad r = 1. \tag{10}$$

For simplicity it has been assumed in Eqs. 8 and 10 that the axial pressure drop along a capillary is small enough that ΔP may be regarded as constant. As discussed elsewhere (3, 7), this assumption is adequate for glomerular capillaries.

The terms involving u and v in Eq. 3 require knowledge of the velocity field. Plasma is to good approximation a Newtonian fluid with constant viscosity (μ) and density (ρ), so that the Navier-Stokes equations are applicable. Just as Eq. 3 represents a balance between convective and diffusive terms in solute transport, the Navier-Stokes equations represent a balance among inertial terms, viscous terms, and pressure gradients in the transport of momentum. The Reynolds number, $Re = RU_0\rho/\mu$, indicates the relative importance of inertial and viscous terms. Since the characteristic velocity (U_0), kinematic viscosity (μ/ρ), and radius (R) for capillary plasma flow are of the order of 10^{-1} cm/s, 10^{-2} cm^2/s, and 10^{-4} cm, respectively, Re is approximately 10^{-3} and the inertial terms may be neglected (22). In addition to this simplification, it is convenient to utilize the stream function, $\psi(r, z)$, which has the property that the velocity vectors are everywhere tangent to lines of constant ψ. The stream function is related to the velocity components as follows:

$$u = -(1/r)(\partial\psi/\partial r), \qquad v = (1/r)(\partial\psi/\partial z). \tag{11}$$

With this definition of ψ, the equations of motion and continuity take the simple form:

$$E^4\psi = 0, \tag{12}$$

where $E^2 = (\partial^2/\partial r^2) - (1/r)(\partial/\partial r) + (\partial^2/\partial z^2)$. Application of the usual no-slip and symmetry conditions for the velocities, together with the ultrafiltration flux equation at the permeable wall, yields the following boundary conditions for ψ:

$$\psi = 0, (\partial\psi/\partial z) = 0 \text{ at } z = 0, \tag{13}$$

$$\psi = -(r^2/2)(\mathrm{d}\beta/\mathrm{d}t), (\partial\psi/\partial z) = 0 \text{ at } z = \beta(t), \tag{14}$$

$$\psi = 0, (1/r)(\partial\psi/\partial r) = \partial^2\psi/\partial r^2 \text{ at } r = 0, \tag{15}$$

$$\partial\psi/\partial r = u_w, (\partial\psi/\partial z) = v_w \text{ at } r = 1. \tag{16}$$

For $\mathrm{d}\beta/\mathrm{d}t$ and v_w both zero, Eqs. 13–16 reduce to the boundary conditions corresponding to no ultrafiltration (18). It is important to note that with vanishingly small Reynolds number, as in the present problem, t does not appear as an independent variable in the momentum equations (see Eq. 12). Consequently, these very low Re flows adjust almost instantaneously to changes in the boundary condi-

tions. The present problem is made time dependent by Eqs. 14 and 16, boundary conditions in which β, $d\beta/dt$, v_w, and u_w all vary slowly with t.

The equations for protein concentration and fluid velocity in the plasma segment have now been specified. Variations in the wall velocity (u_w) and red cell spacing (β) remain to be determined by macroscopic balances. The first of these relates the mean ultrafiltration velocity ($\bar{v}_w$) to the relative velocity of the red cells ($d\beta/dt$):

$$d\beta/dt = -2\beta\bar{v}_w, \ \beta(0) = \beta_0, \tag{17}$$

where $\bar{v}_w$ is defined as:

$$\bar{v}_w = \frac{1}{\beta}\int_0^\beta v_w \, dz. \tag{18}$$

Since it is assumed that no protein is lost through the capillary wall and that the same number of erythrocytes leave the capillary per unit time as enter it, the following relations hold:

$$u_w(t) = 1/\bar{c}(t) = \beta(t)/\beta_0 . \tag{19}$$

The mean protein concentration ($\bar{c}$) is defined as:

$$\bar{c} = \frac{2}{\beta}\int_0^\beta\int_0^1 cr \, dr \, dz. \tag{20}$$

As ultrafiltration proceeds, β decreases (Eq. 17), and therefore $\bar{c}$ increases and u_w decreases (Eq. 19).

The species transport and momentum equations are coupled through the convective terms in Eq. 3 and the velocity boundary condition at the permeable wall, Eq. 16. In addition, two of the boundaries are moving with velocities which are functions of time, given by Eqs. 17 and 19. The numerical solution of these equations is described in the Appendix.[2]

Tube Flow

Solution of the equations for species and momentum transport in an ultrafiltering tube without red cells is relatively straightforward. The usual stationary coordinate system will be employed here, with the coordinate x again denoting axial distance measured from the entrance to the ultrafiltering tube. The other symbols will likewise remain unchanged. The steady-state species transport equation applicable to tube flow for high Pe is:

$$Pe\left[u\frac{\partial c}{\partial x} + v\frac{\partial c}{\partial r}\right] = \frac{\partial^2 c}{\partial r^2} + \frac{1}{r}\frac{\partial c}{\partial r}. \tag{21}$$

[2] Copies of the Appendix are available from the authors.

The axial diffusion term, $\partial^2 c/\partial x^2$, is $0(Pe^{-2})$ and has therefore been neglected (23). The boundary conditions at $r = 0$ and $r = 1$ are given again by Eqs. 6 and 10, and the inlet condition (corresponding to Eq. 4) is:

$$c = 1 \text{ at } x = 0. \tag{22}$$

The solution to Eq. 21 is facilitated by the fact that explicit formulas for the velocity components, u and v, may be obtained:

$$u = 2\bar{u}(1 - r^2), \tag{23}$$

$$v = v_w r(2 - r^2), \tag{24}$$

$$\bar{u} = 1 - 2\int_0^x v_w \, dx'. \tag{25}$$

Eqs. 23 and 24 are valid for small Re, small Pe_w/Pe, and long tubes, conditions fulfilled in the present problem. The derivation of Eqs. 23 and 24, together with a description of the numerical solution to Eq. 21, may be found in the Appendix.[2] Using a different method of derivation, Kozinski et al. (24) obtained velocity profiles similar to Eqs. 23 and 24.

Calculation of Effective Hydraulic Permeability

The effective hydraulic permeability (k) is defined using a recently described model of glomerular ultrafiltration (9), in which protein concentration is a function only of the axial distance coordinate (x), and in which concentration polarization is therefore neglected. To allow comparison with the bolus flow and tube flow models, this one-dimensional model will be applied here to a single idealized capillary, with ΔP assumed to be constant. The solution to the differential equation expressing conservation of fluid and protein for the one-dimensional model, evaluated at the end of the capillary ($x = L/R$), is (9):

$$\frac{A_1}{2}\ln\left|\frac{\phi^2}{1 - A_1\phi - A_2\phi^2}\right| - \frac{1}{\phi} + \left(\frac{A_1^2 + 2A_2}{2\sqrt{A_1^2 + 4A_2}}\right)\ln\left|\frac{\sqrt{A_1^2 + 4A_2} + A_1 + 2A_2\phi}{\sqrt{A_1^2 + 4A_2} - A_1 - 2A_2\phi}\right| = \frac{2k\Delta P}{U_0}\left(\frac{L}{R}\right) \tag{26}$$

where $A_1 = a_1 C_0/\Delta P$, $A_2 = a_2 C_0^2/\Delta P$, and L/R is the ratio of capillary length to radius. ϕ is a function of the amount of fluid filtered:

$$\begin{aligned} \phi &= 1/\bar{u} \quad \text{(tube flow)} \\ &= 1/u_w \quad \text{(bolus flow)} \end{aligned} \tag{27}$$

For given sets of input parameters, ϕ is calculated from either the bolus model or tube flow model, allowing determination of k from Eq. 26. Comparison of this value of k with the value of k_m assumed as an input parameter in the polarization calculations provides a sensitive estimate of the effect of concentration polarization on this ultrafiltration process. It must hold that $k/k_m \leq 1$, equality between k and k_m occurring only in the ideal case where diffusion is so rapid as to prevent the establishment of radial concentration gradients.

RESULTS

Range of Parameters

Both polarization models involve the dimensionless parameters Pe, Pe_w, b_1, and b_2, while in addition, the bolus model requires specification of the initial cell spacing, β_0. The ranges of these parameters to be considered are shown in Table I, together with the corresponding dimensional quantities. Flow velocities and dimensions of single glomerular capillaries, not yet measured in vivo, have been assumed to be similar to those found in extrarenal capillaries (25–28). The value in Table I for C_0, the afferent arteriolar or systemic protein concentration, is typical of that measured in the rat (2–6, 8). The membrane hydraulic permeability, k_m, was taken to equal the effective permeability previously calculated from micropuncture data (5, 8), while ΔP was chosen to bracket the range of pressures observed in the rat between normal (2–4, 6, 8) and very high (5, 8) glomerular plasma flow rates. The range for β_0 was selected arbitrarily. In addition to the quantities in Table I, a fixed aspect ratio of $L/R = 25$ was used for comparison of the bolus and tube flow models, corresponding to a capillary length (L) roughly equivalent to glomerular diameter in the rat (29). The exact value assumed for L/R will be seen to have little effect on the results obtained for k/k_m.

TABLE I

SUMMARY OF PARAMETERS USED IN CALCULATIONS

Dimensional quantities	
R/D	200–1,000 s/cm
U_0	0.05–0.12 cm/s
ΔP	35.0–49.7 mm Hg
C_0	6.0 g/100 ml
k_m	4.1×10^{-5} cm/(s·mm Hg)
Dimensionless quantities	
Pe	10–120
Pe_w	0.120–1.20
b_1	3.58–5.08
b_2	1.08
β_0	0.50–2.0

Extent of Concentration Polarization

Concentration profiles for the tube flow model will be considered first. Fig. 2 shows radial concentration profiles at several positions along an ultrafiltering tube for intermediate values of the parameters in Table I. At any axial position, the protein concentration at the wall ($r = 1$) is greater than at the centerline ($r = 0$), as required by the balance between convective transport of protein toward the wall and diffusion away from it. At any radial position, the concentration increases with axial distance (x), a result of the cumulative removal of ultrafiltrate. The progressive increase in the concentration at the wall with x diminishes the ultrafiltration rate by increasing the osmotic pressure, and thereby decreases the radial concentration gradient at the wall (Eq. 10) as x becomes large. This gradient would vanish if ultrafiltration were allowed to proceed until $\Delta\pi = \Delta P$. Larger values of Pe_w than in Fig. 2 increase the radial concentration gradients and smaller values of Pe_w reduce them, but the qualitative behavior of the concentration profiles is similar.

The distribution of protein concentration in the bolus model may be understood by first considering the nature of the fluid motion. Typical streamlines tracing the motion of fluid elements at a given instant ($t = 10$) are shown in Fig. 3. Note that from the definition of ψ in Eq. 11, fluid velocity is greatest when the streamlines are spaced most closely. The left and right panels are for $\beta_0 = 1.0$ and $\beta_0 = 0.5$, respectively, with all other parameters the same. In both cases the translation of the capillary wall (lower boundary) from right to left causes a clockwise circulation, shown by the closed streamlines. The vortex center is near $r = 0.8$ for $\beta_0 = 1.0$ and $r = 0.9$ for $\beta_0 = 0.5$. In addition, there are streamlines which originate at the surface of red cell 2 (right boundary in both cases) and terminate at the capillary wall, indicating that red cell 2 is being displaced toward red cell 1 (the latter assumed to be stationary) as a result of fluid loss by ultrafiltration. The most striking difference between the two flow patterns in Fig. 3 is in the size of the vortices, the closed streamline region occupying essentially the whole cross section for $\beta_0 = 1.0$ but only slightly more than half for $\beta_0 = 0.5$. It is interesting to note that for $\beta_0 = 0.5$ and no fluid loss, a second vortex is found near the tube centerline (18), but that this weaker vortex is eliminated by a small amount of ultrafiltration (Fig. 3, right). Comparison of the streamline patterns in Fig. 3 leads one to expect that the fluid motion in the $\beta_0 = 1.0$ case will be more effective in transporting protein away from the wall than for $\beta_0 = 0.5$. Thus, it is reasonable to expect more concentration polarization for $\beta_0 = 0.5$ than for $\beta_0 = 1.0$, all other parameters the same.

Fig. 4 shows lines of constant concentration corresponding to the streamlines in Fig. 3. Concentrations adjacent to the capillary wall (lower boundary) are, of course, greater than those at the axis (upper boundary). Furthermore, as protein is convected from right to left along the wall, concentration increases until a maximum is reached at $r = 1$, $z = 0$. In the tube flow case, small radial velocities are always directed toward the wall, and transport of protein away from the wall can

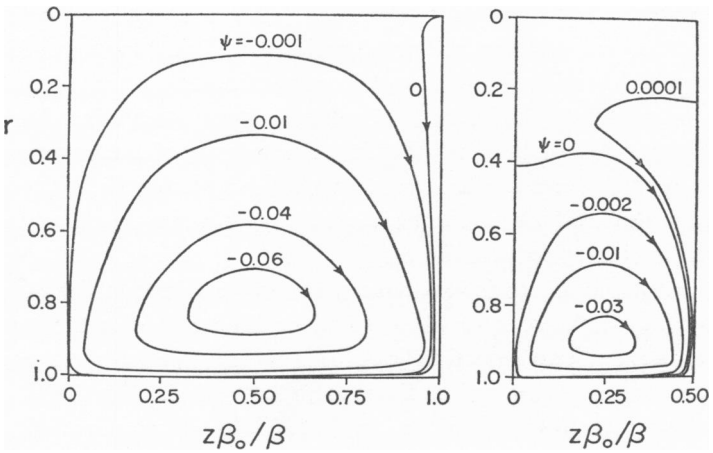

FIGURE 3 Bolus model streamlines for two different initial cell spacings at $t = 10$ ($x = 9.5$). $\beta = 0.905$ (left) and 0.454 (right), $Pe = 50$, $Pe_w = 0.301$, $b_1 = 3.58$, and $b_2 = 1.08$.

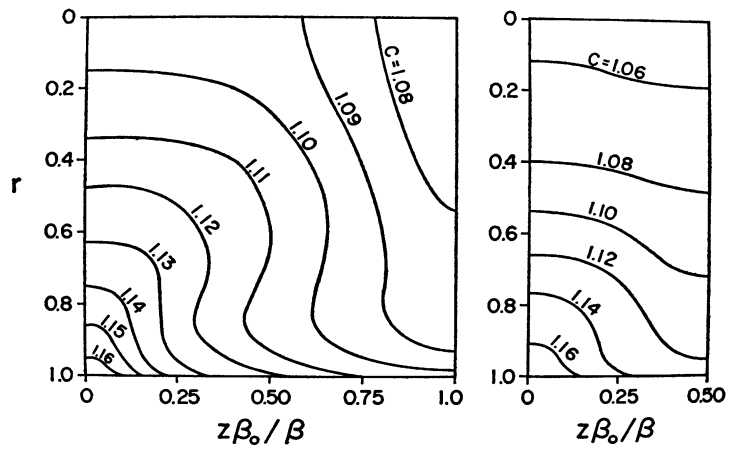

FIGURE 4 Bolus model concentration lines for two different initial cell spacings. Parameters are given in legend to Fig. 3.

therefore occur only by diffusion. This contrasts with the situation shown in Figs. 3 and 4 for the bolus model, in which the vortex motion augments diffusive transport near $z = 0$, the region where the flow turns away from the wall, while it opposes diffusion near $z = \beta$. The interaction between convection and diffusion of protein can be further appreciated by realizing that, in the absence of any circulation within the bolus, protein concentration would be independent of z. That is, if $u_w = 0$, lines of constant concentration would be straight lines parallel to the tube wall (concentric cylinders in three dimensions). This pattern is approximated only by the $c = 1.06$ and 1.08 lines for $\beta_0 = 0.5$ (right panel of Fig. 4), which are in a region

of relatively stagnant fluid (compare with Fig. 3). Despite values of Pe of the order of 100 in this study, no substantial "core" region was found in which diffusion was essentially negligible and in which lines of constant concentration corresponded to streamlines, in contrast with studies of related closed streamline flows (30, 31). This behavior may be attributed to the time dependence of the concentration field in the present problem, and the fact that the only steady state which may be achieved is the trivial case of uniform concentration at large t, when $\Delta\pi$ closely approaches ΔP and ultrafiltration effectively ceases.

Fig. 4 indicates that there is less concentration polarization for $\beta_0 = 1.0$ than for $\beta_0 = 0.5$, in accordance with what would be expected from the streamlines in Fig. 3. Streamlines and concentration lines for $\beta_0 = 2.0$, not shown, are qualitatively similar to those for $\beta_0 = 1.0$, and indicate even less polarization for this larger cell spacing. For purposes of comparison, it is useful to define a quantity (θ) which measures the extent of concentration polarization at any point along the capillary:

$$\theta = (c_w/\bar{c}) - 1. \tag{28}$$

For the tube flow model, c_w is the wall concentration and $\bar{c}$ is the radial average concentration at a given point x. To obtain $\theta(x)$ for the bolus flow model, $\bar{c}$ is calculated from Eq. 20, and c_w is found by averaging $c(1, z)$ from $z = 0$ to $z = \beta$. Note that $\theta \geq 0$, equality holding only in the absence of polarization. For both polarization models θ initially equals 0, increases to a maximum after a short distance (typically near $x = 5$), and then gradually declines. In other words, there is net accumulation of protein at the wall for small values of x, where ultrafiltration rates are highest, followed by dissipation of these concentration gradients as ultrafiltration diminishes due to increased $\Delta\pi$. For the parameter values used to obtain Figs. 2–4, θ over most of the capillary length is between 0.04 and 0.06 for the tube model, between 0.02 and 0.04 for the bolus model with $\beta_0 = 0.5$, and between 0.01 and 0.03 for the bolus model with $\beta = 1.0$. Thus, the circulatory flow created by the red cells in the bolus model is sufficient in this case to reduce the extent of polarization to roughly one-half of that computed for the tube model. Even with the tube model, however, the wall concentration exceeds the radial average concentration by a maximum of only 6–7%.

Concentration polarization leads to higher osmotic pressures than would otherwise exist, and thus lower ultrafiltration rates. This is illustrated in Fig. 5, in which filtration fraction, the fraction of the initial flow which has been filtered up to a given point, is plotted for parameters corresponding to Figs. 2–4. The curve labeled "one-dimensional model" was computed assuming no radial concentration gradients (as described elsewhere [9]), and therefore represents the maximum filtration fraction achievable for the given input parameters. As expected from the preceding discussion, the tube model filtration fractions are smallest. It is interesting to note that while c_w exceeded $\bar{c}$ for the tube model by an average of only about 5% under

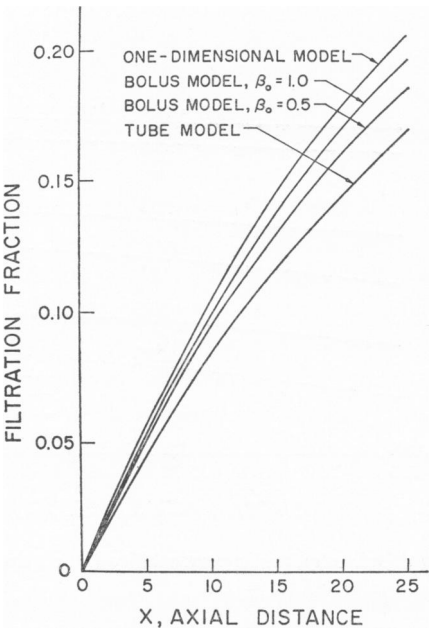

FIGURE 5 Comparison of filtration fractions for one-dimensional model (9), bolus model, and tube model. Parameters are the same as those for Figs. 2–4.

these conditions, the tube model filtration fraction at $x = 25$ is some 18% less than that computed in the absence of polarization.

Effective Hydraulic Permeability

The effects of different values of β_0 in the bolus model have now been discussed in some detail. The other parameters varied in the polarization calculations were Pe, Pe_w, and b_1, corresponding to variations in the dimensional quantities R/D, U_0, and ΔP. In general, the extent of polarization increases in either model as R/D or ΔP are increased, while changes in U_0 have relatively little effect. Since the primary goal of this study was to assess how much the effective hydraulic permeability (k) and actual membrane permeability (k_m) may differ as a result of concentration polarization, the results for all parameter combinations are best summarized in terms of k/k_m, values for which are given in Fig. 6 for the tube model and Fig. 7 for the bolus model. If there were no polarization, k/k_m would equal 1.0. For the inputs used in Figs. 2–5 ($R/D = 500$ s/cm, $\Delta P = 35$ mm Hg, and $U_0 = 0.1$ cm/s), thought to be representative of glomerular capillaries, k/k_m is roughly 0.7 for tube flow (Fig. 6) and 0.9 for bolus flow (Fig. 7). Recalling that values of θ under these same conditions were less than 0.07, it is apparent that even modest amounts of polarization may significantly affect k/k_m.

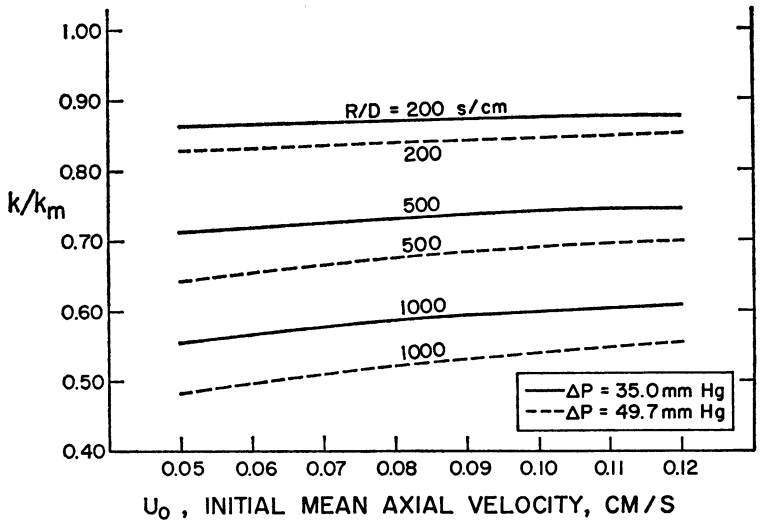

FIGURE 6 Normalized effective hydraulic permeability (k/k_m) from tube flow model as a function of U_0, R/D, and ΔP for $L/R = 25$.

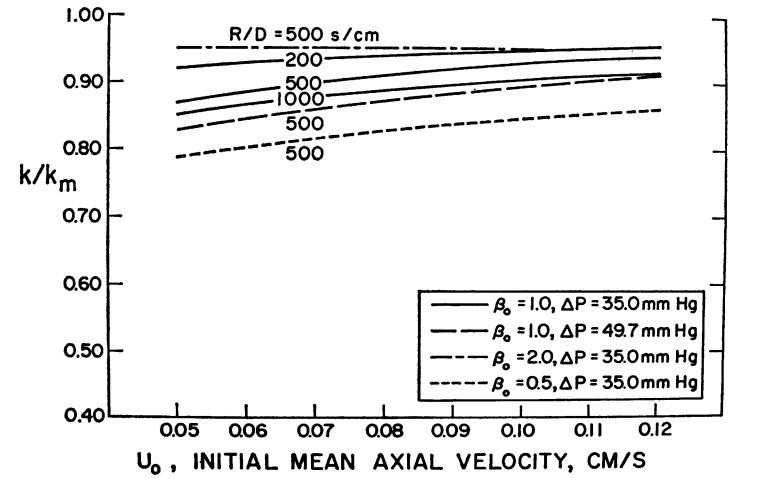

FIGURE 7 Normalized effective hydraulic permeability (k/k_m) from bolus flow model as a function of U_0, R/D, and ΔP for $L/R = 25$.

An interesting finding shown in Figs. 6 and 7 is the relative insensitivity of k to changes in U_0, k/k_m increasing by less than about 10% for all cases as U_0 is increased over more than a twofold range. This is in close agreement with experimental results in the rat, in which k (assuming glomerular capillary surface area to be constant) was found not to vary over an approximately twofold range of glomerular plasma flow rates (5). Over this range of flow rates, ΔP was observed to

increase (on average) from 39 to 44 mm Hg (5). As indicated in Figs. 6 and 7, slight increases in ΔP together with increased flow (U_0) are predicted by either model to leave k virtually unchanged, the effects of simultaneous increases in ΔP and U_0 tending to oppose one another.

It is also possible from Figs. 6 and 7 to determine the sensitivity of k/k_m to the assumed value of the aspect ratio, L/R. Of central importance is that the axial coordinates of both the one-dimensional and tube flow models may be transformed to eliminate the axial velocity parameter from the respective sets of equations (23). For example, in the tube flow case, a new axial coordinate ($\hat{x}$) may be defined such that $\hat{x} = x/Pe$. This, together with letting $\hat{v} = vPe$, eliminates Pe from Eq. 21, demonstrating that increases in axial distance (x) are exactly equivalent to decreases in initial mean velocity (U_0), as long as $\hat{x}$ is unchanged. For instance, this implies that for the tube flow model, k/k_m for $U_0 = 0.10$ cm/s and $L/R = 50$ is identical to that for $U_0 = 0.05$ cm/s and $L/R = 25$. The insensitivity of k/k_m to U_0 shown in Fig. 6 therefore implies a similar insensitivity to the assumed value for L/R, a fortunate result, since L/R is not known precisely. A more complete discussion of this finding is given elsewhere (23). For the bolus model, the equivalence of changes in U_0 and x could not be demonstrated by coordinate transformations, but was tested by comparing the value of u_w at $L/R = 12.5$ and $U_0 = 0.05$ cm/s with that at $L/R = 25.0$ and $U_0 = 0.10$ cm/s for the six parameter combinations represented by curves in Fig. 7. The corresponding values of u_w were found to differ by an average of only 0.3 % (range: 0–0.9 %), indicating that in the bolus model as well as the tube model, proportional increases in U_0 and x leave filtration fraction and k/k_m essentially unchanged. Thus, for both polarization models, the insensitivity of k/k_m to changes in U_0 (Figs. 6 and 7) implies a similar insensitivity to L/R, so that the exact values of U_0 and L/R are not of great importance in estimating k/k_m.

DISCUSSION

The possible influence of hemodynamics on the exchange of substances through capillary walls has been the subject of a number of investigations. Prothero and Burton (14), recognizing that in many capillaries erythrocytes travel singly, separated by segments of plasma, termed this regime "bolus flow" and attempted to estimate the enhancement of gaseous transport due to plasma motion by analogy with large-scale heat transfer experiments. These authors concluded that the circulatory motion within the plasma segments considerably accelerates gaseous equilibration, especially within peripheral capillaries. Aroesty and Gross (17, 32), however, have shown this conclusion to be based on erroneous scaling arguments, and have demonstrated by numerical solution of the momentum and species transport equations (in the absence of transcapillary fluid exchange) that enhanced mixing due to the convective motions of plasma should not appreciably augment trans-

port of dissolved gases. Bugliarello and Hsiao (16) and Lew and Fung (15) also concluded, using less rigorous arguments, that transport of dissolved gases in capillaries must occur primarily by diffusion.

The reason that gas transport should be almost unaffected by plasma motion is that the Péclet number (Pe), which measures the relative importance of convection and diffusion, is only of order unity for species such as CO_2 and O_2 in capillaries. In contrast, the transport of more slowly diffusing species such as proteins, where Pe is of order 10–100, should be considerably enhanced by convection, as pointed out in passing by a number of authors (17, 30, 32–34). The importance of convection to protein transport, however, has previously received little detailed attention. This may be attributed to the fact that modeling of capillary blood flow (for reviews see 32, 35–37) has been concerned primarily with situations where there is little or no ultrafiltration or fluid absorption, and where concentration polarization phenomena are therefore not encountered. The renal glomerular capillaries present an example of a capillary bed where ultrafiltration is both quantitatively large and of physiological importance in the maintenance of extracellular fluid volume and composition. The results of this study show that the secondary motions in plasma induced by red cells may considerably alter the radial distribution of protein within a glomerular capillary, and thereby affect the colloid osmotic pressure. Comparison of bolus and tube flow models of capillary ultrafiltration (with and without idealized red cells, respectively) indicates that the ratio of effective hydraulic permeability (k) to actual membrane hydraulic permeability (k_m) may be increased from 0.7 to 0.9 under typical conditions. This increase in k/k_m results from the circulatory motion of plasma between successive red cells and reflects a decrease in mean colloid osmotic pressure. Both models show k/k_m to be relatively insensitive to plasma flow rate, although k/k_m may be substantially less than unity. This is in agreement with the experimental finding that the glomerular ultrafiltration coefficient, the product of k and capillary surface area, is unchanged by variations in glomerular plasma flow rate (5).

It has been shown theoretically (9) that k (or quantities proportional to k) can be estimated from experimental data only under conditions where filtration pressure equilibrium is not observed, that is, when $\Delta\pi$ is still significantly less than ΔP at the efferent end of the glomerular capillary. Accordingly, calculations in this study were performed using parameter values for which $\Delta\pi$ was always substantially less than ΔP, corresponding to such experimental situations (5, 8). Studies in both rat and monkey, however, show that filtration pressure equilibrium is normally achieved (2–4, 6–8). Although concentration polarization will occur under conditions of filtration pressure equilibrium, except near the efferent end of the capillary where $\Delta\pi \cong \Delta P$, the overall filtration fraction is governed solely by the values of C_0 and ΔP. Consequently, only when filtration pressure equilibrium does not exist will concentration polarization affect the overall filtration fraction.

The bolus model of capillary blood flow employed here represents an extreme simplification of the interactions between red cell and plasma motion. Red cells are flexible and assume a number of complex shapes when passing through small capillaries (32, 37). In addition, even in the narrowest capillaries, there must be some leakage of plasma past red cells. The characteristics of the thin lubrication layer of plasma existing between a red cell and the capillary wall have in fact been the subject of several theoretical studies (34, 38, 39). Allowing for curvature of the red cell surfaces (16) or plasma leakage around the red cells (33), however, have both been shown to have little qualitative effect on the motion throughout most of the plasma segment between idealized cells. In this study it seemed appropriate to examine the bolus configuration as one limiting case, where the red cells completely occlude the capillary (no leakage) and where the vortices between cells presumably have maximum effect on protein concentrations. The tube flow model was adopted as the other limiting case, in which red cells are neglected entirely. It is therefore expected that the actual effects of concentration polarization on capillary ultrafiltration are intermediate between those predicted by these two models. With regard to this point, it should be noted that the tube flow results cannot be achieved by letting $\beta_0 \rightarrow \infty$ in the bolus model, since the initial condition for the bolus model (Eq. 4) is applicable only when $\beta_0 \ll L/R$. That is, initial red cell spacing must be much less than tube length. Since L/R was taken to be 25, values of β_0 not larger than 2.0 were employed.

Caution is advisable in speculating about a possible relationship between capillary hematocrit (different, in general, from systemic hematocrit but presumably related to β_0) and k/k_m, because of the gross approximations inherent in the bolus flow approach and because capillary hematocrits are themselves not routinely measured or well known. It may be briefly noted, however, that the results shown in Fig. 7 do suggest an inverse relationship between k/k_m and capillary hematocrit, over some hematocrit range.

A result of this study which was not anticipated is that protein concentrations at the capillary wall do not greatly exceed the radial average values, even though k/k_m may be substantially less than unity. In the worst cases considered, this difference was a maximum of about 8% for the bolus model and roughly twice that for the tube model. The wall concentration most often exceeded the radial average concentration by less than 5% when averaged along the capillary. For molecular species which are only partially retained by the capillary wall, radial concentration gradients should be less than those for the major plasma proteins (assumed here to be retained completely). The radial concentration gradients for semipermeant species are lessened even further if these species have higher diffusivities in water than that assumed for plasma proteins (7×10^{-7} cm^2/s), a likely possibility since such species would be expected in general to have lower molecular weights than serum albumin. It is therefore entirely justifiable to analyze sieving data of macro-

molecules using one-dimensional models which neglect radial concentration gradients. The present results also emphasize that the one-dimensional model of glomerular ultrafiltration developed previously (9) remains useful, particularly since k is found not to be strongly flow dependent.

Concentration polarization has been discussed primarily as it relates to glomerular ultrafiltration. It is worthwhile to note, however, that polarization effects are also expected for capillaries where there is net fluid absorption, such as renal peritubular capillaries. During fluid absorption, v_w and thus the concentration gradient at the wall (Eq. 7) are negative, so that $c_w < \bar{c}$. As with ultrafiltration, the actual driving force for fluid exchange during absorption is lower than if polarization were absent, so that k/k_m for peritubular capillaries should again be less than unity. Since the protein concentration in the Bowman's space fluid surrounding the glomerular capillary is negligible (40), concentration polarization phenomena can occur only on the blood side of the glomerular capillary wall. Such is not the case for the peritubular capillary, where the protein concentration in the surrounding interstitial fluid may be 2–3 g/100 ml, some 40% of the systemic level (21). Thus, there may be polarization on the blood side of the peritubular capillary wall in the absorption sense ($c_w < \bar{c}$), and polarization on the interstitial side in the ultrafiltration sense ($c_w > \bar{c}$). The possibility of concentration polarization on the interstitial side of a capillary wall, considered recently by Lee (41), complicates the interpretation of effective hydraulic permeability for peritubular and extrarenal capillaries. This is particularly true since experimental difficulties have prevented the pressure and composition of interstitial fluid from being characterized as well as those of Bowman's space or renal tubule fluid (1).

The authors especially thank Dr. G. M. Homsy for his invaluable assistance in the formulation of the numerical methods used in this study.
Grateful acknowledgment is also made to Dr. A. Acrivos for his helpful suggestions and to Ms. Meredith Clark for her expert secretarial assistance.

This study was supported in part by grants from the National Institutes of Health (HE 14945 and AM 13888). Computer time was made available by the School of Engineering, Stanford University.

Dr. Deen is a Postdoctoral Research Fellow of the National Kidney Foundation.

This work was presented in part at the 6th Annual Meeting of the American Society of Nephrology, Washington, D. C., 19 November 1973. (1973. Abstracts of the 6th Annual Meeting, American Society of Nephrology. 30.)

Received for publication 12 November 1973 and in revised form 15 January 1974.

REFERENCES

1. DEEN, W. M., C. R. ROBERTSON, and B. M. BRENNER. 1973. *Circ. Res.* **33**:1.
2. BRENNER, B. M., J. L. TROY, and T. M. DAUGHARTY. 1971. *J. Clin. Invest.* **50**:1776.
3. BRENNER, B. M., J. L. TROY, T. M. DAUGHARTY, W. M. DEEN, and C. R. ROBERTSON. 1972. *Am. J. Physiol.* **223**:1184.
4. ROBERTSON, C. R., W. M. DEEN, J. L. TROY, and B. M. BRENNER. 1972. *Am. J. Physiol.* **223**:1191.

5. DEEN, W. M., J. L. TROY, C. R. ROBERTSON, and B. M. BRENNER. 1973. *J. Clin. Invest.* **52**:1500.
6. DAUGHARTY, T. M., I. F. UEKI, P. F. MERCER, and B. M. BRENNER. *J. Clin. Invest.* 1974. **53**:105.
7. MADDOX, D. A., W. M. DEEN, and B. M. BRENNER. 1974. *Kidney Internatl.* **5**:271.
8. DEEN, W. M., D. A. MADDOX, C. R. ROBERTSON, and B. M. BRENNER. 1974. *Am. J. Physiol.* In press..
9. DEEN, W. M., C. R. ROBERTSON, and B. M. BRENNER. 1972. *Am. J. Physiol.* **223**:1178.
10. BLATT, W. F., A. DRAVID, A. S. MICHAELS, and L. NELSEN. 1970. *In* Membrane Science and Technology. J. E. Flinn, editor. Plenum Press, New York. 47.
11. KOZINSKI, A. A., and E. N. LIGHTFOOT. 1972. *A. I. Chem. Eng. J.* **18**:1030.
12. KOZINSKI, A. A., and E. N. LIGHTFOOT. 1971. *A. I. Chem. Eng. J.* **17**:81.
13. GILL, W. N., L. J. DERZANSKY, and M. R. DOSHI. 1971. *In* Surface and Colloid Science. E. Matijevic, editor. John Wiley & Sons, Inc., New York. **4**:261.
14. PROTHERO, J., and A. C. BURTON. 1961. *Biophys. J.* **1**:565.
15. LEW, H. S., and Y. C. FUNG. 1969. *Biorheology.* **6**:109.
16. BUGLIARELLO, G., and G. C. HSIAO. 1970. *Biorheology.* **7**:5.
17. AROESTY, J., and J. F. GROSS. 1970. *Microvasc. Res.* **2**:247.
18. DUDA, J. L., and J. S. VRENTAS. 1971. *J. Fluid Mech.* **45**:247.
19. BIRD, R. B., W. E. STEWART, and E. N. LIGHTFOOT. 1960. Transport Phenomena. John Wiley & Sons, Inc., New York. 559.
20. KELLER, K. H., E. R. CANALES, and S. I. YUM. 1971. *J. Phys. Chem.* **75**:379.
21. DEEN, W. M., C. R. ROBERTSON, and B. M. BRENNER. 1973. *Biophys. J.* **13**:340.
22. HAPPEL, J., and H. BRENNER. 1965. Low Reynolds Number Hydrodynamics. Prentice-Hall, Inc., Englewood Cliffs, N. J. 40.
23. DEEN, W. M. 1973. Ph.D. Thesis. Stanford University, Stanford, Calif.
24. KOZINSKI, A. A., F. P. SCHMIDT, and E. N. LIGHTFOOT. 1970. *Ind. Eng. Chem. Fundam.* **9**:502.
25. INTAGLIETTA, M., and B. W. ZWEIFACH. 1971. *Circ. Res.* **28**:593.
26. SMAJE, L., B. W. ZWEIFACH, and M. INTAGLIETTA. 1970. *Microvasc. Res.* **2**:96.
27. INTAGLIETTA, M., D. R. RICHARDSON, and W. R. TOMPKINS. 1971. *Am. J. Physiol.* **221**:922.
28. ERIKSSON, E., and R. MYRHAGE. 1972. *Acta Physiol. Scand.* **86**:211.
29. KIRKMAN, H., and R. E. STOWELL. 1942. *Anat. Rec.* **82**:373.
30. DUDA, J. L., and J. S. VRENTAS. 1971. *J. Fluid Mech.* **45**:261.
31. PAN, Y.-F., and A. ACRIVOS. 1968. *Int. J. Heat Mass Transfer.* **11**:439.
32. GROSS, J. F., and J. AROESTY. 1972. *Biorheology.* **9**:225.
33. FITZ-GERALD, J. M. 1972. *J. Fluid Mech.* **51**:463.
34. LIGHTHILL, M. J. 1968. *J. Fluid Mech.* **34**:113.
35. LIGHTHILL, M. J. 1972. *J. Fluid Mech.* **52**:475.
36. FUNG, Y. C. 1969. *J. Biomech.* **2**:353.
37. FUNG, Y. C., and B. W. ZWEIFACH. 1971. *Annu. Rev. Fluid Mech.* **3**:189.
38. FITZ-GERALD, J. M. 1969. *Proc. Roy. Soc. Lond. B.* **174**:193.
39. LIN, K. L., L. LOPEZ, and J. D. HELLUMS. 1973. *Microvasc. Res.* **5**:7.
40. GAIZUTIS, M., A. J. PESCE, and J. E. LEWY. 1972. *Microchem. J.* **17**:327.
41. LEE, J.-S. 1972. *J. Appl. Physiol.* **32**:254.